Diagn Interv Radiol 2026; DOI: 10.4274/dir.2026.263859

NEURORADIOLOGY

ORIGINAL ARTICLE

The hematoma measurement accuracy of dual-energy computed tomography angiography in spontaneous intracerebral hemorrhage

Baoteng Zhang
Qingjing Huang
Feijian Wu
Suying Wu
Jianfang Huang
Zhihua Lu

The First Hospital of Putian City, Department of Radiology, Putian, China

Corresponding author: Zhihua Lu

E-mail: luzhuren0438@163.com

Received 09 January 2026; revision requested 24 February 2026; accepted 08 April 2026.

Epub: 01.06.2026

DOI: 10.4274/dir.2026.263859

PURPOSE

To investigate the accuracy of hematoma volume (V), surface area (S), and surface regularity (SR) measured on dual-energy computed tomography angiography (DECTA), using non-contrast computed tomography (NCCT) as the reference standard.

METHODS

A total of 129 patients with spontaneous intracerebral hemorrhage (sICH) who underwent both NCCT and DECTA scans were retrospectively studied. Patients were stratified by V: Group 1 (< 30 mL), Group 2 (30–60 mL), and Group 3 (> 60 mL); and by morphology: regular, irregular, and lobular. DECTA data were post-processed to generate conventional computed tomography angiography (CTA) and 60 keV virtual monoenergetic imaging (VMI). These, along with NCCT images, were imported into 3D Slicer software to obtain V and S; SR was subsequently calculated. Deviation percentages (ΔV, ΔS, ΔSR) of conventional CTA and 60 keV VMI relative to NCCT were calculated. We assessed correlations using simple linear regression, compared different modalities with unpaired t-tests or Mann–Whitney U tests, evaluated agreement via Bland–Altman analysis, and compared deviation percentages across groups using one-way analysis of variance or Kruskal–Wallis H tests. Inter-reader consistency was assessed using the intraclass correlation coefficient (ICC).

RESULTS

The average V was 28.86±24.15 mL. All ICCs were excellent (0.991–0.999). Strong correlations were found for V and S between conventional CTA/60 keV VMI and NCCT (r: 0.987–0.996). Bland–Altman analysis for V showed mean biases of 0.21 mL (conventional CTA) and −0.04 mL (60 keV VMI) against NCCT, with 95% limits of agreement of −4.72 to 5.14 mL and −4.51 to 4.43 mL, respectively. However, SR values from both conventional CTA and 60 keV VMI were significantly lower than those from NCCT (all $P < 0.001$). In volume-based stratification, no significant differences in ΔS (conventional CTA) or ΔV, ΔS, and ΔSR (60 keV VMI) were found among groups (all $P \geq 0.410$). For conventional CTA, ΔV was significantly smaller in Group 3 (> 60 mL) than in Group 1 (3.07% vs. 5.57%, adjusted $P = 0.047$), whereas ΔSR was larger (13.26% vs. 9.88%, adjusted $P = 0.040$). Morphology-based stratification revealed no significant differences in ΔV, ΔS, or ΔSR across groups for either modality (all P values ≥ 0.085).

CONCLUSION

Hematoma volume measurements from DECTA show good agreement with NCCT measurements, suggesting potential utility for follow-up assessment in certain clinical scenarios. However, DECTA-derived SR measurements are significantly lower than those from NCCT. Volume measurement accuracy of conventional CTA was higher for large hematomas (> 60 mL).

CLINICAL SIGNIFICANCE

Accurate hematoma measurement is crucial for prognosis and management in sICH. This study indicates that V measurements from DECTA are comparable to those from NCCT in certain clinical scenarios, offering potential added value when CTA is clinically indicated.

KEYWORDS

Dual-energy, computed tomography angiography, virtual monoenergetic imaging, intracerebral hemorrhage, hematoma volume

You may cite this article as: Zhang B, Huang Q, Wu F, Wu S, Huang J, Lu Z. The hematoma measurement accuracy of dual-energy computed tomography angiography in spontaneous intracerebral hemorrhage. *Diagn Interv Radiol*. 01 June 2026 DOI: 10.4274/dir.2026.263859 [Epub Ahead of Print].

Spontaneous intracerebral hemorrhage (sICH) is a neurological emergency characterized by non-traumatic rupture of cerebral vessels and subsequent hematoma formation within the parenchyma, associated with high mortality and morbidity.[1] Hematoma location, hematoma volume (V), hematoma expansion (HE), and perihematomal edema are independent predictors of functional outcomes and mortality.[2-4] Thus, accurate hematoma assessment is vital for treatment planning and prognosis prediction.

Neuroimaging plays a pivotal role in the diagnosis of intracerebral hemorrhage (ICH) and monitoring its progression. Non-contrast computed tomography (NCCT), favored for its speed and diagnostic accuracy, is the first-line modality. Various NCCT signs based on hematoma density and shape are used to predict HE.[5,6] Hematoma morphology is a recognized prognostic factor for HE, with visual scales categorizing hematomas by morphological characteristics.[7-9] Irregular margins have been linked to HE and worse outcomes. To reduce subjective bias, Oge et al.[10] investigated surface regularity (SR), calculated from volume and surface area (S), and its relationship to HE, finding that hematomas evolve into more irregular shapes with significantly reduced SR during follow-up.

Computed tomography (CT) angiography (CTA) is used to identify underlying etiologies (e.g., aneurysms or vascular malformations). The "spot sign" on CTA also predicts HE.[11] Dual-energy CT has advanced rapidly and is widely applied in clinical neuroradiology. Dual-energy CTA (DECTA) provides not only conventional CTA data but also additional parameters such as iodine maps, virtual non-contrast (VNC) images, and virtual monoenergetic imaging (VMI), potentially enhancing ICH detection and HE prediction.[12] In practice, neuroradiologists need to measure V on CTA to assess progression, yet the accuracy of such cross-modal measurements remains unclear.

Main points

- Hematoma volume and surface area measured on dual-energy computed tomography angiography (DECTA)-derived images from conventional computed tomography angiography (CTA) and 60 keV virtual monoenergetic imaging show excellent correlation with non-contrast computed tomography measurements.
- The DECTA approach has potential value for the follow-up assessment of hematoma volume in certain clinical scenarios.
- Conventional CTA is more accurate for volume measurements of large hematomas (> 60 mL) than for small- and medium-sized hematomas.

Hematoma volume is a key indicator of early mortality and 90-day neurological recovery.[2,13] three dimensional (3D) Slicer, a free, open-source image analysis platform, facilitates V measurement via semi-automated segmentation and 3D reconstruction based on radiodensity, offering accurate and reproducible assessment independent of hematoma shape or location.[14,15]

This study used 3D Slicer software to retrospectively evaluate the accuracy of V, S, and SR measurements on DECTA relative to NCCT.

Methods

Study population and grouping

This retrospective study recruited patients diagnosed with sICH at the First Hospital of Putian City between January 2020 and June 2024. Inclusion criteria: (1) CT scans performed within 6 hours of symptom onset, with NCCT and DECTA performed sequentially within 30 minutes; (2) a single parenchymal hematoma with volume ≥ 5 mL; (3) no pregnancy, iodine contrast allergy, or severe cardiopulmonary/renal dysfunction. Exclusion criteria: (1) hematoma outline obscured by intratumoral hemorrhage or hemorrhagic transformation of ischemic infarction, and (2) poor image quality or incomplete clinical data. Figure 1 shows the patient selection flowchart. The Ethics Committee of the First Hospital of Putian City approved the study (protocol number: 2022-037, date: 28.12.2022); written informed consent was waived due to the retrospective and anonymized design of this study.

Based on NCCT-measured volume using 3D Slicer, patients were stratified as Group 1 (< 30 mL), Group 2 (30-60 mL), and Group 3 (> 60 mL). Based on the hematoma's maximal slice, morphology was categorized as regular (round/ellipsoid, smooth margins), irregular (frayed margins), or lobular.[16]

Image acquisition and reconstruction

All scans were performed on a third-generation dual-source CT scanner (SOMATOM Force; Siemens Healthineers, Erlangen, Germany); NCCT was followed by DECTA. Scanning range: skull base to vertex; NCCT parameters: tube voltage: 120 kV, pitch: 0.6 mm; DECTA parameters: tube voltages: 80 kV and 150 kV, pitch: 0.7 mm. Reconstruction: matrix: 512 × 512, slice thickness: 1.0 mm, spacing: 0.7 mm, and convolution kernel: Qr40. Automated tube current modulation (CareDose4D) was used.

Iopromide (370 mgI/mL; Bayer, Berlin, Germany) was injected via the antecubital vein at 1.0 mL/kg (4.5 mL/s), followed by a 40 mL saline flush. Bolus tracking in the ascending aorta [100 Hounsfield unit (HU) threshold + 4s delay] triggered scanning.

The 80 kV, Sn150 kV, and blended 115 kV (50/50 mix, approximating conventional 120 kV) images were processed on a Siemens workstation (syngo.via VB10B). Based on literature supporting improved head/neck CTA quality at 60 keV,[17,18] 60 keV VMI images were reconstructed; NCCT, conventional CTA, and

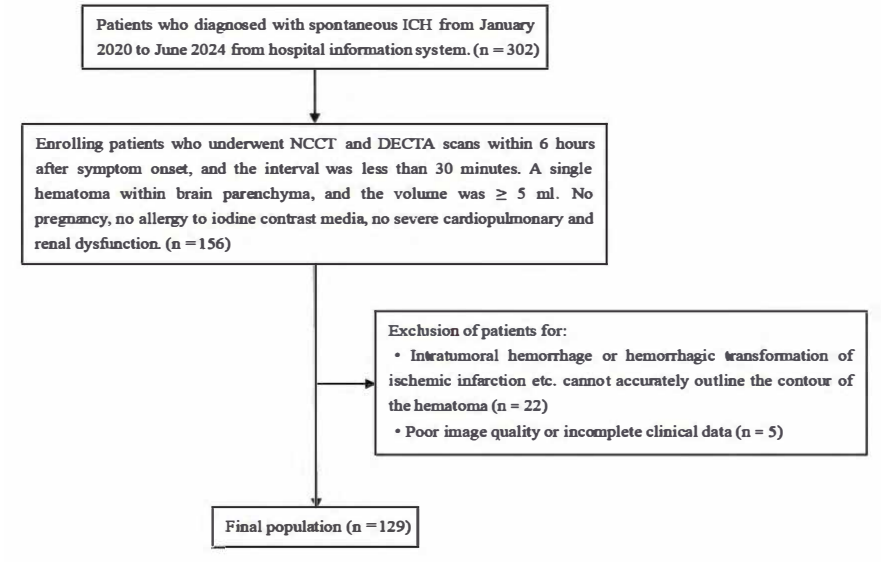

Figure 1. The flowchart of the inclusion and exclusion criteria for the study. ICH, intracerebral hemorrhage; NCCT, non-contrast computed tomography; DECTA, dual-energy computed tomography angiography.

60 keV VMI sets were used for subsequent analysis.

Hematoma measurement

DICOM images were analyzed using 3D Slicer (v5.7.0; Brigham and Women's Hospital, Boston, MA, USA). Two well-trained radiologists, blinded to clinical data, semi-automatically delineated hematoma outlines (threshold: 40-100 HU) with manual correction. The software calculated V and S; the average of the two radiologists' measurements was used (Figure 2); SR was calculated as follows: $SR = 6\sqrt{\pi}(\frac{V}{\sqrt{S^3}})$, ranging from 0 (irregular) to 1 (spherical) (10). Deviation percentages (ΔV, ΔS, and ΔSR) for conventional CTA and 60 keV VMI relative to NCCT were computed using the following formula:

$$\Delta V = \frac{|V_{test} - V_{control}|}{V_{control}} \times 100\%$$

Statistical analysis

Analyses were performed using SPSS Statistics (v25.0; IBM, Armonk, NY, USA) and GraphPad Prism (v8.0.2; GraphPad Software, San Diego, CA, USA). Continuous variables are expressed as mean ± SD or median (interquartile range) based on normality (Kolmogorov–Smirnov test). Categorical variables are presented as n (%). Simple linear regression assessed correlations. Inter-modality comparisons used unpaired t-tests or Mann–Whitney U tests. Agreement was evaluated via Bland–Altman analysis. Deviation percentages across groups were compared using one-way analysis of variance or the Kruskal–Wallis H test, with post-hoc Dunn–Bonferroni tests. Box plots were used to visualize the distribution of deviation percentages for conventional CTA and 60 keV VMI. The intraclass correlation coefficient (ICC) assessed inter-reader consistency: 0.41–0.60 (moderate), 0.61–0.80 (strong), 0.81–1.00 (excellent). A P value < 0.05 was considered statistically significant.

Results

The study included 129 patients, including 86 men (66.7%) and 43 women (33.3%), with a mean age of 61.47 ± 11.06 years. The interval from symptom onset to scan was 3.12 ± 1.80 hours. Volume groups: Group 1: 80 (62.0%), Group 2: 33 (25.6%), Group 3: 16 (12.4%). Morphology: regular: 29 (22.5%), irregular: 63 (48.8%), lobular: 37 (28.7%). Location: deep (basal ganglia/thalamus): 74 (57.4%), lobar: 53 (41.1%), infratentorial: 2 (1.6%). Inter-reader ICCs for V and S across all modalities were excellent (0.991–0.999) (Table 1).

Strong linear correlations existed for V and S between conventional CTA/60 keV VMI and NCCT (all P < 0.001, r: 0.987-0.996) (Figures 3a1–b2), with no significant difference between correlation coefficients (all P ≥ 0.359). However, SR values from both conventional CTA and 60 keV VMI were significantly lower than those from NCCT (all P < 0.001). Bland–Altman analysis (Figure 4) showed for conventional CTA vs. NCCT: mean bias (V: 0.21 mL, S: 5.22 mm^2, SR: −0.06) with 95% limits of agreement (LoA) of −4.72, 5.14 mL, −10.70, 21.14 mm^2, −0.19, 0.08. For 60 keV VMI vs. NCCT: mean bias (V: −0.04 mL, S: 3.21 mm^2, SR: −0.05) with 95% LoA of −4.51, 4.43 mL, −8.45, 14.88 mm^2, −0.19, 0.10.

The results of volume-stratified analysis were as follows: (1) ΔV (Conventional CTA): Group 1: 5.57%, Group 2: 5.21%, Group 3: 3.07%; ΔV in Group 3 was significantly lower than in Group 1 (z = −2.419, adjusted P = 0.047, Figure 5a); (2) ΔV (60 keV VMI): no significant difference among groups (5.23%, 4.66%, 3.40%; H = 1.785, P = 0.410, Figure 5b); (3) ΔS (Conventional CTA and 60 keV VMI): no significant differences among volume groups (H = 1.665/0.381, P = 0.435/0.827) (Figure 6a, b); (4) ΔSR (Conventional CTA): Group 1: 9.88%, Group 2: 7.47%, Group 3: 13.26%; ΔSR in Group 3 was significantly higher than in Group 2 (z = 2.475, adjusted P = 0.040) (Figure 7a); (5) ΔSR (60 keV VMI): no significant difference among groups (7.35%, 4.88%, 8.75%; H = 0.657, P = 0.720) (Figure 7b).

The results of the morphology-stratified analysis indicated no significant differences in ΔV, ΔS, or ΔSR among the regular, irregular, and lobular groups for either conventional CTA or 60 keV VMI (all H ≥ 1.243, all P ≥ 0.085) (Figures 8–10).

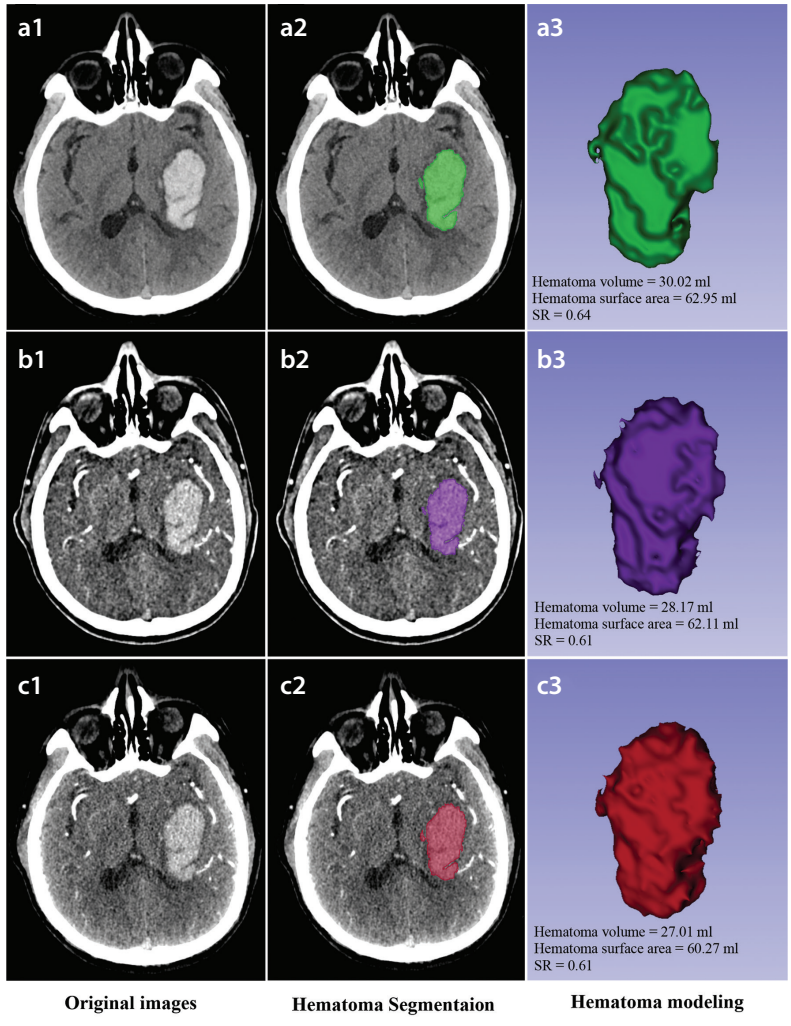

Figure 2. Hematoma segmentation and modeling of a patient with hemorrhage in the left basal ganglia region. Figures **a1–a3** illustrate the hematoma segmentation and modeling results on NCCT using 3D Slicer software; Figures **b1–b3** and **c1–c3** depict the segmentation and modeling results for the same patient on conventional CTA and 60 keV VMI, respectively. Hematoma volume and surface area are displayed below the 3D models, and SR values were calculated accordingly. NCCT, non-contrast computed tomography; CTA, computed tomography angiography; SR, surface regularity; 3D, three dimensional; VMI, virtual monoenergetic imaging.

Table 1. The inter-reader ICC values of hematoma volume and surface area measured on NCCT, conventional CTA, and 60 keV VMI

Parameters / Modalities	NCCT	Conventional CTA	60 keV VMI
Volume	0.999	0.999	0.991
Surface area	0.998	0.998	0.998

Please note that these values were inter-reader ICC values. NCCT, non-contrast computed tomography; CTA, computed tomography angiography; VMI, virtual monoenergetic imaging; ICC, intraclass correlation coefficient.

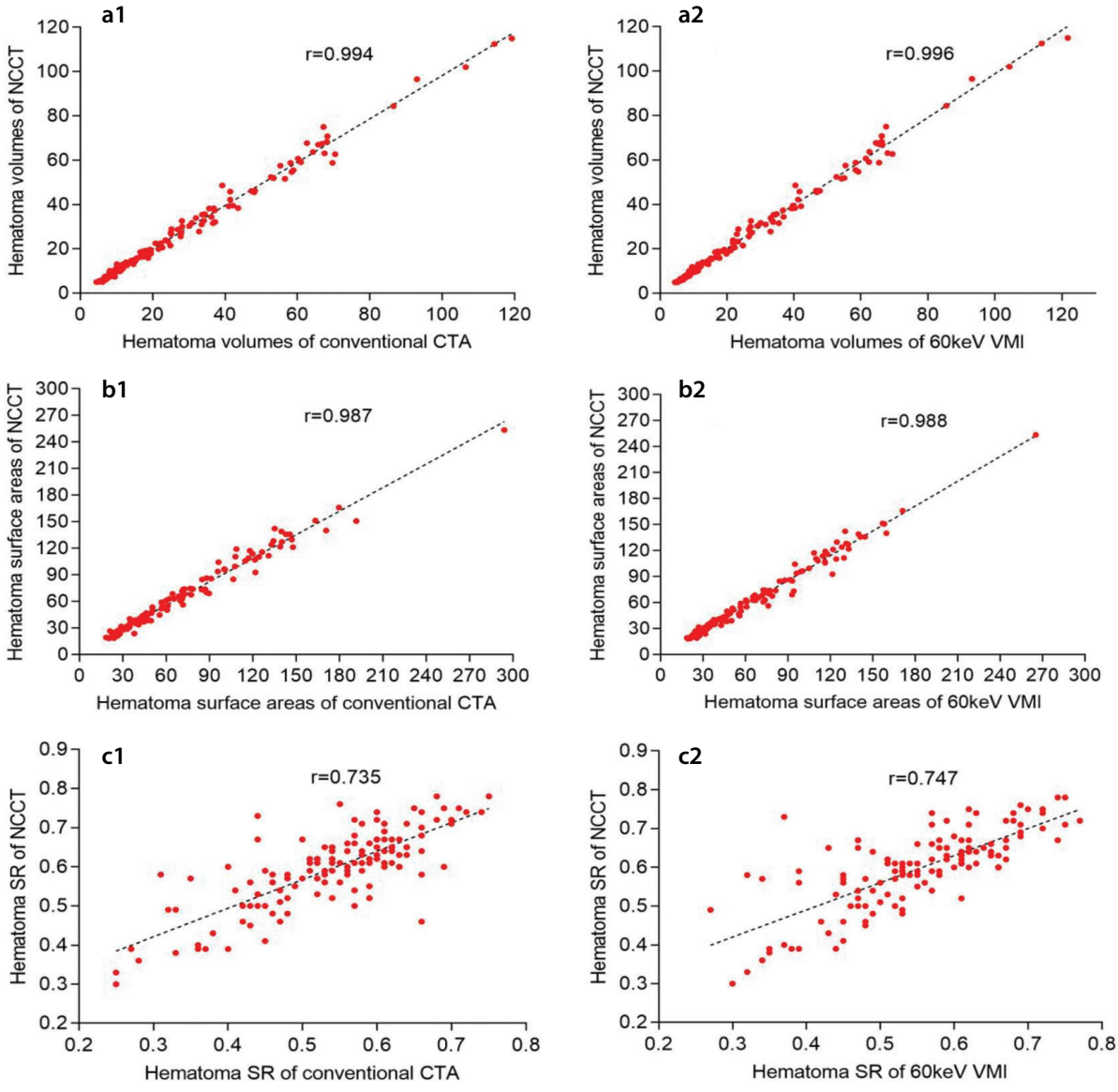

Figure 3. Simple linear correlation analysis between the volume, surface area, and SR of conventional CTA, 60 keV VMI, and those of NCCT. Figures **a1–a2** and **b1–b2** demonstrate that the volume and surface area of conventional CTA and 60 keV VMI are linearly correlated with those of NCCT, respectively (r approaching 1); Figures **c1–c2** show a moderate linear correlation between the SR of conventional CTA, 60 keV VMI, and that of NCCT. NCCT, non-contrast computed tomography; CTA, computed tomography angiography; SR, surface regularity; VMI, virtual monoenergetic imaging.

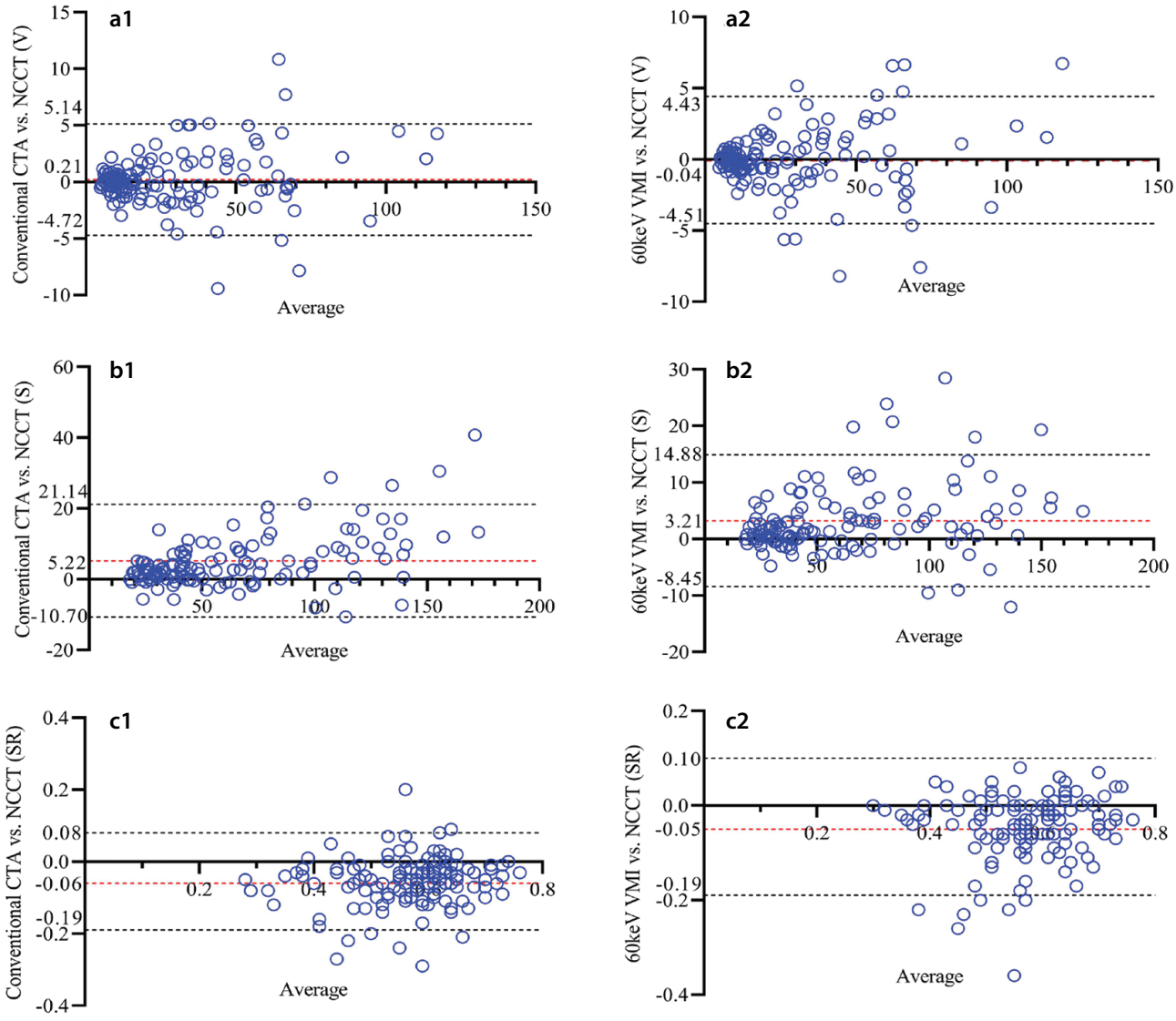

Figure 4. Bland–Altman scatter plots for V, S, and SR of conventional CTA/60 keV VMI vs. NCCT. Dashed red lines represent the mean bias of measurement deviations. Dashed black lines represent the 95% limits of agreement. CTA, computed tomography angiography; NCCT, non-contrast computed tomography; V, hematoma volume; S, surface area; SR, surface regularity; VMI, virtual monoenergetic imaging.

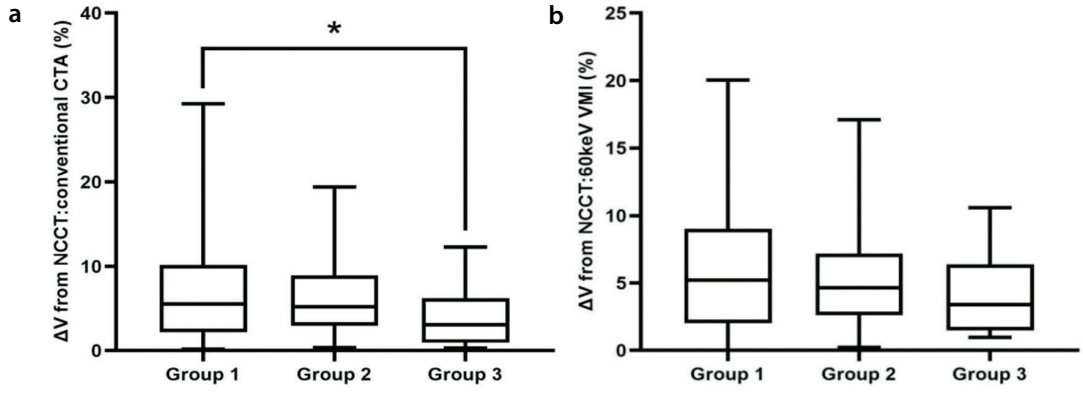

Figure 5. Comparison of ΔV among different hematoma volume groups in conventional CTA (**a**) and 60 keV VMI (**b**). The box plots display the upper quartiles, lower quartiles, and medians. Group 1: < 30 mL; Group 2: 30–60 mL; Group 3: >60 mL. *indicates statistically significant difference. CTA, computed tomography angiography; VMI, virtual monoenergetic imaging; ΔV, deviation percentage in hematoma volume.

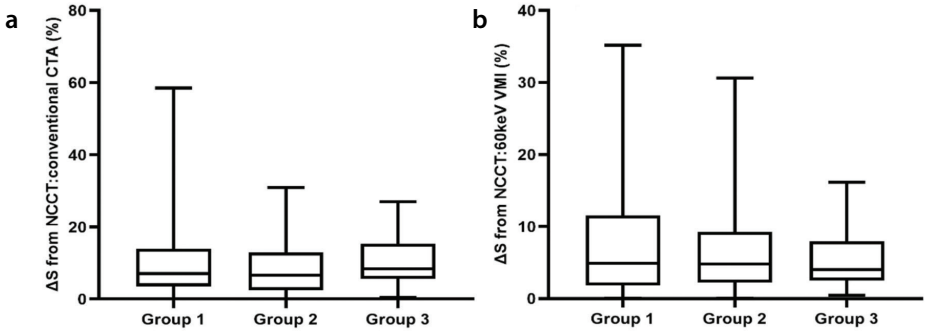

Figure 6. Comparison of ΔS among different hematoma volume groups in conventional CTA (**a**) and 60 keV VMI (**b**). The box plots display the upper quartiles, lower quartiles, and medians. Group 1: < 30 mL; Group 2: 30–60 mL; Group 3: > 60 mL. CTA, computed tomography angiography; VMI, virtual monoenergetic imaging; ΔS, deviation percentage in surface area.

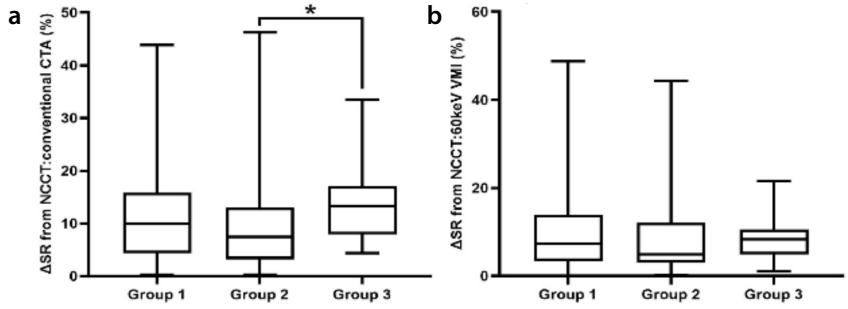

Figure 7. Comparison of ΔSR among different hematoma volume groups in conventional CTA (**a**) and 60 keV VMI (**b**). The box plots display the upper quartiles, lower quartiles, and medians. Group 1: < 30 mL; Group 2: 30–60 mL; Group 3: > 60 mL. *indicates statistically significant difference. CTA, computed tomography angiography; VMI, virtual monoenergetic imaging; ΔSR, deviation percentage in surface regularity.

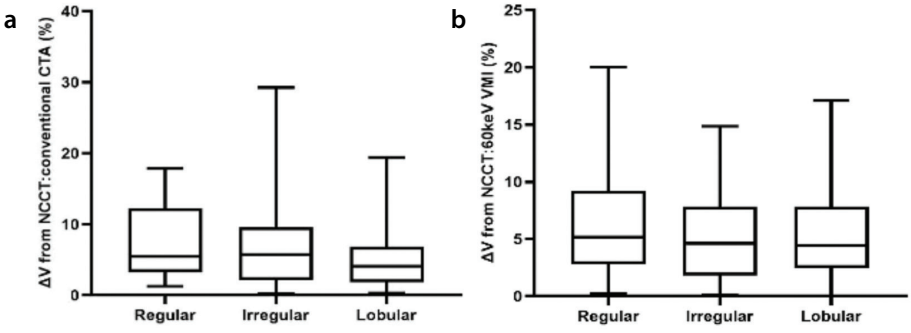

Figure 8. Comparison of ΔV among different hematoma morphology groups in conventional CTA (**a**) and 60 keV VMI (**b**). The box plots display the upper quartiles, lower quartiles, and medians. CTA, computed tomography angiography; VMI, virtual monoenergetic imaging; ΔV, deviation percentage in hematoma volume.

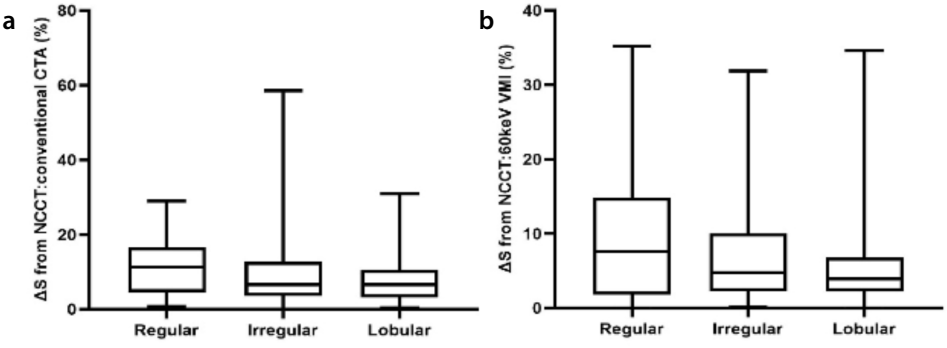

Figure 9. Comparison of ΔS among different hematoma morphology groups in conventional CTA (**a**) and 60 keV VMI (**b**). The box plots display the upper quartiles, lower quartiles, and medians. CTA, computed tomography angiography; VMI, virtual monoenergetic imaging; ΔS, deviation percentage in surface area.

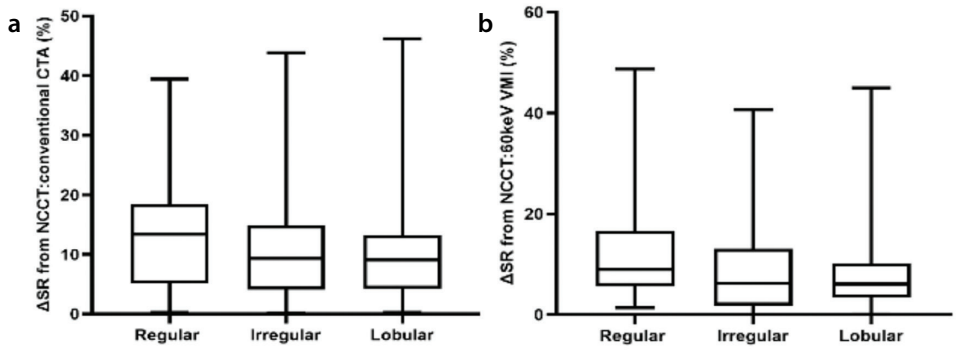

Figure 10. Comparison of ΔSR among different hematoma morphology groups in conventional CTA (**a**) and 60 keV VMI (**b**). The box plots display the upper quartiles, lower quartiles, and medians. CTA, computed tomography angiography; VMI, virtual monoenergetic imaging; ΔSR, deviation percentage in surface regularity.

Discussion

This study evaluated the accuracy of hematoma measurements on DECTA. To our knowledge, it is among the first to comprehensively analyze the accuracy of hematoma V, S, and SR measurements on conventional CTA and 60 keV VMI from DECTA compared with NCCT. We observed excellent linear correlations for V and S between conventional CTA/60 keV VMI and NCCT, regardless of V and shape. Bland–Altman analysis confirmed good agreement for V, with minimal mean bias and 95% LoA ranges narrower than established thresholds for HE (6 mL)[5] and surgical decision-making (30/60 mL).[13] However, SR was consistently underestimated on DECTA. In volume-based analysis, ΔS for conventional CTA and ΔV/ΔS/ΔSR for 60 keV VMI showed no significant differences across groups, suggesting error magnitudes may scale similarly with volume. Notably, for conventional CTA, the estimation error of V was smaller for large hematomas (> 60 mL), whereas the estimation error of SR was larger. No significant differences were found across morphology groups for any parameter.

Accurate measurement of V is crucial for assessing prognosis and planning treatment.[2] Although NCCT is the standard, clinicians may need to assess V on other modalities, and its accuracy remains unclear. Schlunk et al.[19] reported that CTA and magnetic resonance imaging could significantly over- or underestimate volume compared with post-contrast CT, considered the most accurate modality. In contrast, our study found no significant systematic bias in volume measurements between DECTA and NCCT. This discrepancy may be due to Schlunk et al.[19]'s smaller sample size (CTA: n = 20) or methodological differences, including the use of DECTA with advanced post-processing.

CTA provides additional diagnostic value (e.g., detecting etiologies and the spot sign). Our study demonstrated that the narrow 95% LoA range for volume measurement on DECTA (approximately ± 5 mL) was lower than the 6 mL threshold for HE diagnosis and the 30/60 mL thresholds for surgical decision-making. Therefore, V measured on DECTA may be comparable to that measured on NCCT in certain clinical scenarios, thereby adding clinical value for patients undergoing CTA.

Although hematoma surface properties contain information on growth dynamics,[5] they are less studied. Fisher's "domino" model suggests vessel shearing causes irregular growth.[5] As a quantitative 3D morphology metric (adapted from tumor imaging),[20] SR has been linked to HE dynamics.[10] Our finding of significantly lower SR on DECTA indicates that SR reproducibility across these modalities is inferior to size-based metrics (V, S), possibly due to contrast enhancement affecting margin delineation. Therefore, the value of SR measured on contrast-enhanced images requires further investigation.

Our study has several limitations. First, the retrospective design and moderate sample size may limit generalizability. Second, we focused on conventional CTA and 60 keV VMI; VNC images, which may more closely approximate NCCT, were not evaluated and warrant future study. Finally, intraventricular hemorrhage cases were excluded, which merits separate investigation.

In conclusion, V measurements from DECTA show good agreement with those of NCCT, indicating potential utility for follow-up assessment in specific clinical scenarios. However, DECTA tends to underestimate SR compared with NCCT. Furthermore, conventional CTA derived from DECTA demonstrated higher volumetric accuracy for large hematomas (> 60 mL) compared with smaller ones.

Footnotes

Conflict of interest disclosure

The authors declared no conflicts of interest.

Funding

This work was supported by the Fujian Provincial Science and Technology Department, Fujian, China [grant number 2023J011727].

References

1. Mazzoleni V, Padovani A, Morotti A. Emergency management of intracerebral hemorrhage. *J Crit Care*. 2023;74:154232. [Crossref]
2. Teo KC, Fong SM, Leung WCY, et al. Location-specific hematoma volume cutoff and clinical outcomes in intracerebral hemorrhage. *Stroke*. 2023;54(6):1548-1557. [Crossref]
3. Huang YW, Huang HL, Li ZP, Yin XS. Research advances in imaging markers for predicting hematoma expansion in intracerebral hemorrhage: a narrative review. *Front Neurol*. 2023;14:1176390. [Crossref]
4. Cliteur MP, Sondag L, Cunningham L, et al. The association between perihaematomal oedema and functional outcome after spontaneous intracerebral haemorrhage: a systematic review and meta-analysis. *Eur Stroke J*. 2023;8(2):423-433. [Crossref]
5. Lv XN, Deng L, Yang WS, Wei X, Li Q. Computed tomography imaging predictors of intracerebral hemorrhage expansion. *Curr Neurol Neurosci Rep*. 2021;21(5):22. [Crossref]
6. Song L, Qiu X, Zhang C, et al. Combining non-contrast CT signs with onset-to-imaging time to predict the evolution of intracerebral hemorrhage. *Korean J Radiol*. 2024;25(2):166-178. [Crossref]

7. Wang CW, Liu YJ, Lee YH, et al. Hematoma shape, hematoma size, Glasgow coma scale score and ICH score: which predicts the 30-day mortality better for intracerebral hematoma? *PLoS One*. 2014;9(7):e102326. [Crossref]
8. Blacquiere D, Demchuk AM, Al-Hazzaa M, et al. Intracerebral hematoma morphologic appearance on noncontrast computed tomography predicts significant hematoma expansion. *Stroke*. 2015;46(11):3111-3116. [Crossref]
9. Delcourt C, Zhang S, Arima H, et al. Significance of hematoma shape and density in intracerebral hemorrhage: the intensive blood pressure reduction in acute intracerebral hemorrhage trial study. *Stroke*. 2016;47(5):1227-1232. [Crossref]
10. Oge DD, Topcuoglu MA, Gocmen R, Arsava EM. The dynamics of hematoma surface regularity and hematoma expansion in acute intracerebral hemorrhage. *J Clin Neurosci*. 2020;74:160-163. [Crossref]
11. Hiramatsu M, Haruma J, Hishikawa T, Sugiu K, Date I. *No Shinkei Geka*. 2021;49(2):284-292. [Crossref]
12. Tran NA, Sodickson AD, Gupta R, Potter CA. Clinical applications of dual-energy computed tomography in neuroradiology. *Semin Ultrasound CT MR*. 2022;43(4):280-292. [Crossref]
13. Hemphill JC 3rd, Greenberg SM, Anderson CS, et al. Guidelines for the management of spontaneous intracerebral hemorrhage: a guideline for healthcare professionals from the American Heart Association/American Stroke Association. *Stroke*. 2015;46(7):2032-2060. [Crossref]
14. Fedorov A, Beichel R, Kalpathy-Cramer J, et al. 3D Slicer as an image computing platform for the Quantitative Imaging Network. *Magn Reson Imaging*. 2012;30(9):1323-1341. [Crossref]
15. Xu X, Chen X, Zhang J, et al. Comparison of the Tada formula with software slicer: precise and low-cost method for volume assessment of intracerebral hematoma. *Stroke*. 2014;45(11):3433-3435. [Crossref]
16. Chen M, Li Z, Ding J, Lu X, Cheng Y, Lin J. Comparison of common methods for precision volume measurement of hematoma. *Comput Math Methods Med*. 2020;2020:6930836. [Crossref]
17. Schneider D, Apfaltrer P, Sudarski S, et al. Optimization of kiloelectron volt settings in cerebral and cervical dual-energy CT angiography determined with virtual monoenergetic imaging. *Acad Radiol*. 2014;21(4):431-436. [Crossref]
18. Wichmann JL, Nöske EM, Kraft J, et al. Virtual monoenergetic dual-energy computed tomography: optimization of kiloelectron volt settings in head and neck cancer. *Invest Radiol*. 2014;49(11):735-741. [Crossref]
19. Schlunk F, Kuthe J, Harmel P, et al. Volumetric accuracy of different imaging modalities in acute intracerebral hemorrhage. *BMC Med Imaging*. 2022;22(1):9. [Crossref]
20. Pérez-Beteta J, Molina-García D, Ortiz-Alhambra JA, et al. Tumor surface regularity at MR imaging predicts survival and response to surgery in patients with glioblastoma. *Radiology*. 2018;288(1):218-225. [Crossref]